

## SMART SENSOR FOR ENHANCEMENT OF A MULTI-SPINDLE AUTOMATIC LATHE THERMAL ERROR COMPENSATION MODEL

O. Horejs<sup>1\*</sup>, M. Mares<sup>1</sup>, A. Mlcoch<sup>2</sup>

<sup>1</sup>Czech Technical University in Prague, Faculty of Mechanical Engineering, Department of Production Machines and Equipment (RCMT), Prague, Czech Republic

<sup>2</sup>TAJMAC-ZPS, a. s., MORI-SAY Division, Zlin, Czech Republic

\*Corresponding author; e-mail: O.Horejs@rcmt.cvut.cz

### Abstract

The development of a smart sensor is proposed to improve the thermal error compensation model of a multi-spindle automatic lathe. The smart sensor is capable of gathering real-time information about rotating spindle drum temperatures. Thereafter, the temperature obtained by the smart sensor is applied as input to the thermal error compensation model based on the transfer function instead of an indigenous temperature measured on the stationary part of the multi-spindle automatic lathe. Using spindle drum temperature as the model input increases the prediction of thermal displacements in the X-axis by 16%.

### Keywords:

Smart sensor; Multi-spindle automatic lathe; Thermal error; Industry 4.0; Accuracy; Compensation;

## 1 INTRODUCTION

In recent years, the introduction of German Industry 4.0 [Lasi 2014] and other national policies [Li 2018] have rendered the intelligent manufacturing a topic of heightened interest. In the context of Industry 4.0, manufacturing systems are updated on an intelligent level. Intelligent manufacturing takes advantage of advanced information and manufacturing technologies to achieve flexible, smart, and reconfigurable manufacturing processes to address a dynamic and global market. Smart sensors, which do not just collect data but can also interpret and communicate it, are the crucial technological driving force behind the development and integral element of the Industry 4.0 concept. Furthermore, out of the various machine tool error sources, thermal errors account for 40–70% of total errors [Mayr 2012]. Therefore, it is important to control and reduce thermal errors to improve the accuracy of precision machine tools. Compensation of thermally induced displacements at the tool centre point (TCP) is one of the most widely employed techniques to reduce these thermal errors because of its cost-effectiveness and ease of implementation. Thus, real-time compensation of thermal errors is an important part of the intelligent functions of modern machine tools [Liu 2019].

The main aim of this paper is to improve the indigenous thermal error compensation model of a multi-spindle automatic lathe [Mares 2014] via a novel smart sensor. The indigenous thermal compensation of a six-spindle automatic lathe is based on transfer function (TF) modelling [Horejs 2010]. Generally, the TF-based compensation technique is seamlessly applied on milling machines.

Milling machine thermal error models can rely on sufficient isolation of dominant heat sources from one another, which makes it possible to resolve each heat source impact on machine tool thermal behaviour separately, with subsequent superposition. Thus, the principle behind the compensation technique lies in the partial linearisation of the thermal issues, with the help of an equation system consisting of linear parametric models, see [Mares 2020]. Excitation in the TF is ordinarily only one temperature measured close to the relevant heat source. The basic TF model concept has already been introduced for different machine tool structures (3-axis, 4-axis, and 5-axis), e.g., [Horejs 2012], [Horejs 2013], [Horejs 2014], [Mares 2020].

In contrast to milling machines, a multi-spindle automatic lathe with several workpiece spindle units is a mechanically complicated machine tool with several heat sources influencing one another. This results in very complex thermal behaviour with problematic prediction of thermal errors, especially the thermal error in the X-axis, which negatively affects the diameters of the machined parts. Moreover, the temperature information on the main heat sources is limited due to the spindle drum rotation, which complicates the placement of temperature probes on the spindle drum. Consequently, application of the above-mentioned modelling approach is unsuitable. Instead of separate solutions for each heat source and subsequent superposition of heat sources solutions, it is suitable to consider the multi-spindle automatic lathe thermal behaviour as one complex heat source.

To improve the accuracy of the compensation model, a smart sensor capable of gathering real-time information about the rotating spindle drum temperatures was developed. Thereafter, a spindle drum temperature obtained by the smart sensor is employed as input to the existing thermal error compensation model based on the TF instead of a temperature measured on the stationary part of the multi-spindle automatic lathe.

## 2 THERMAL ERROR COMPENSATION MODEL

### 2.1 Six-spindle automatic lathe

The research relates to a multi-spindle automatic lathe with several workpiece spindle units, in particular the MORI-SAY TMZ642CNC numerically controlled six-spindle automatic lathe produced by TAJMAC-ZPS, see Fig. 1. Workpiece spindle units are arranged around a central axis, which can be driven rotationally and advanced from one machining position (MP) to the next MP.

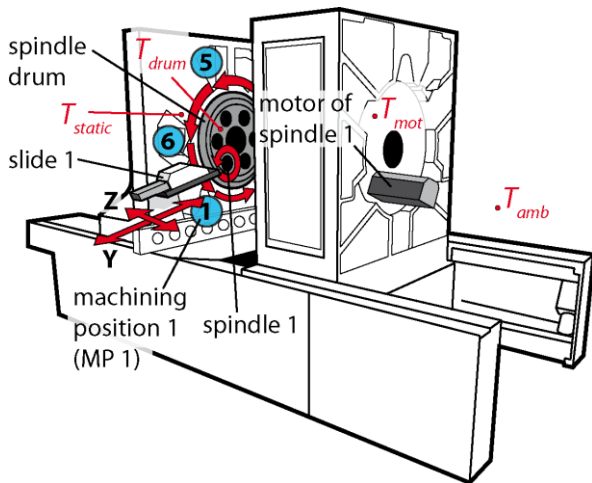


Fig. 1: A general overview of the MORI-SAY TMZ642CNC six-spindle automatic lathe (the scheme of the machine is simplified to show only feed drives in machining position 1 (MP1) for image clarity).

Generally, multi-spindle automatic lathes have a spindle drum, mounted on a machine frame, on which the workpiece spindles are mounted at rigidly fixed angles equal to one another and onto which they are brought into various MPs by advancing the spindle drum. The innovative technical solution allows the speed of each spindle to be controlled separately and the power of each AC spindle motor to be calibrated in accordance with the requirements of the specific machining operations performed for each customer. At the same time, the absolute independence of each spindle makes it possible to perform any type of machining, including machining operations requiring spindle stopping or C-axis spindle orientation, thus making the six-spindle automatic lathe a real and complete turning and milling centre. The six-spindle automatic lathe is equipped with two SINUMERIK 840D solution line CNC control systems to control up to 48 CNC controlled axes (a total of 26 CNC controlled axes and 22 additional CNC controlled axes for optional equipment control) [TAJMAC-ZPS 2020].

### 2.2 Compensation model based on the TF

The described MORI-SAY TMZ642CNC six-spindle automatic lathe has quite a small workspace in comparison with conventional medium-sized CNC milling machines. Therefore, the volumetric variance of the thermal errors is not an issue. Moreover, the thermally induced displacements are negligible in the Y-direction and

Z-direction. Thus, the only notable direction to compensate is the X-direction (workpiece diameters that are machined at different MPs of the six-spindle automatic lathe, see Fig. 1).

Dynamic TF-based modelling was applied to predict thermally induced displacements in the X-direction. The TF contains the nature of the heat transfer principles. Thus, the calibration of the empirical parameters is simple, in addition the model is more reliable with untested inputs, and it can even be used reliably to extrapolate data since it forces the data to conform to the same mathematical form as the real process.

A discrete TF was used to describe the link between the excitation (temperature) and its response (thermally induced displacements in the X-direction  $\delta_{x,i}$ ), equations (1) and (2)

$$y(t) = \varepsilon \cdot u(t) + e(t), \quad (1)$$

$$y(t) = \frac{a_n z^{-n} + \dots + a_1 z^{-1} + a_0 z^0}{b_m z^{-m} + \dots + b_1 z^{-1} + b_0 z^0} \cdot u(t); \text{ where } m > n. \quad (2)$$

The vector  $u(t)$  in (1) and (2) is the TF input in the time domain,  $y(t)$  is the output vector in the time domain,  $\varepsilon$  represents the TF in the time domain,  $e(t)$  is the disturbance value (neglected),  $a_n$  are the calibration coefficients of the TF input,  $b_m$  are the calibration coefficients of the TF output,  $n$  is the order of the TF numerator,  $m$  is the order of the TF denominator, and  $z$  is a complex number.

The difference form of a discrete TF (the generally suitable form for modern machine tool control systems using their programming languages) in the time domain is introduced in equation (3)

$$y(k) = \frac{u(k-n)a_n + \dots + u(k-1)a_1 + u(k)a_0}{b_0} - \frac{y(k-m)b_m + \dots + y(k-1)b_1}{b_0}, \quad (3)$$

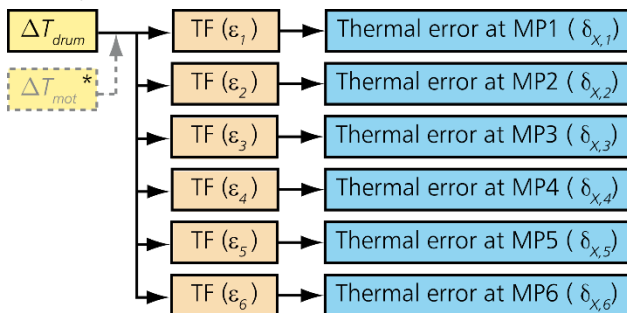
where  $k$  represents the examined time instant and  $k-n$  ( $k-m$ ) is the  $n$ -multiple ( $m$ -multiple) delay in the sampling frequency of the measured input vector (simulated output vector). The linear parametric models of ARX (autoregressive with external input) or OE (output error) identifying structures were used for an estimation of the TF coefficients. The stability of each TF and the relationship between the thermo-mechanical system input and output described by the TF are examined through a linear time invariant (LTI) step response [Ljung 2020].

### 2.3 Compensation model inputs

The six-spindle automatic lathe was equipped with 29 resistance temperature sensors (RTD, Pt100, Class A, 3850 ppm/K) see [Mares 2014]. Firstly, sensors were placed on the stationary parts of the machine and different mathematical models based on the TF according to equation (3) were developed to compensate the thermal errors in the X-direction of the six-spindle automatic lathe, see [Mareš 2014]. As mentioned above, the excitation in the TF  $\varepsilon$  is ordinarily the temperature measured close to the relevant heat source (the heat source whose impact on the overall thermal error at the TCP the particular TF describes). This paper aims to adapt this approach to six-spindle automatic lathes with complicated thermal behaviour. Therefore, the approximation quality of different compensation TF models with only one input temperature measured on the stationary part of the lathe was investigated. The TF model with temperature placed at the

flange of the spindle motor  $T_{mot}$  has the best approximation quality (see Fig. 1). Nevertheless, the prediction of thermal errors in the X-direction based on the TF model with temperature  $T_{mot}$  was still not satisfactory from the machine tool builder's point of view. The presumed reason for the lower approximation quality of the developed compensation model based on the TF is that the key temperature of the rotating spindle drum is inaccessible (not measured).

Secondly, to improve the accuracy and robustness of the compensation model using the TF, a smart sensor capable of gathering real-time information about the rotating spindle drum temperature ( $T_{drum}$ ) was developed. Subsequently, the spindle drum temperature  $T_{drum}$  was employed as TF model input. The scheme of the thermal error compensation model based on the TF is shown in Fig. 2. Each thermal error at the MP in the X-direction is predicted by an individual TF, e.g., the thermal error at MP1 in X-direction ( $\delta_{x,1}$ ) by TF denominated as  $\varepsilon_1$ , etc.



\* The original TF model using temperature measured on the stationary part ( $T_{mot}$ , see Fig.1) as the input.

Fig. 2: The scheme of the thermal error compensation model based on the TF.

A comparison of the two TF compensation models using one temperature as input, measured on the stationary part at the flange of the spindle motor ( $T_{mot}$ ) or measured on the rotating spindle drum ( $T_{drum}$ ), is carried out in Section 5.

### 3 SMART SENSOR

#### 3.1 Smart sensor design

As the spindle drum rotates to reciprocally change the relative position of the spindles and workpieces, it is not very feasible to use standard temperature measurements with contact temperature sensors with a cable (e.g., RTD, thermocouple) or noncontact temperature measurements via an infrared sensor due to the absence of free mounting space. Moreover, in the case of an infrared sensor only the surface temperature, which can be significantly influenced by flood cooling (cutting oil), is measured. Therefore, it was necessary to develop a smart sensor (a special measuring system including sensors, microprocessor, and communication technology) for wireless measurement of spindle drum temperature. To integrate the smart sensor into the spindle drum, the structure of the spindle drum was modified. Furthermore, the six-spindle automatic lathe was equipped with a number of special construction and measurement elements including contactless power supply systems.

The fundamental requirements for the smart sensor are:

- Fully applicable for industrial application on multi-spindle automatic lathes.
- Ingress protection IP 65 to IP68 according to the IEC 60529 standard [IEC 60529 2013] for critical parts of the

smart sensor, which can be in contact with the cutting oil.

- Industrial communication of the smart sensor with the machine tool control system (e.g., PROFIBUS).
- Additional network communication between the smart sensor and the data acquisition system (programmable automation controller NI cRIO-9014 produced by National Instruments) [National Instruments 2016].
- Temperature accuracy  $\pm 0.25$  °C (typical) from  $-40$  °C to  $125$  °C.

#### 3.2 Hardware and communication design

The smart sensor consists of three main parts:

1. temperature sensors;
2. a measuring and transmitting unit;
3. a receiving and integration unit;

##### Temperature sensors

Digital MCP9808 temperature sensors produced by Microchip Technology Inc. [Microchip 2011] were used for sensing spindle drum temperatures. The digital temperature sensor is inserted into a special housing, which is designed as the brass screw. The manufactured housings of the temperature sensors are mounted into the spindle drum on the side of the working space, and six housings in total are positioned between the workpiece spindles (two sensors are visible in Fig. 3). The sensors are equally placed in the middle between each spindle ( $60^\circ$  between adjacent sensors, see Fig. 3).

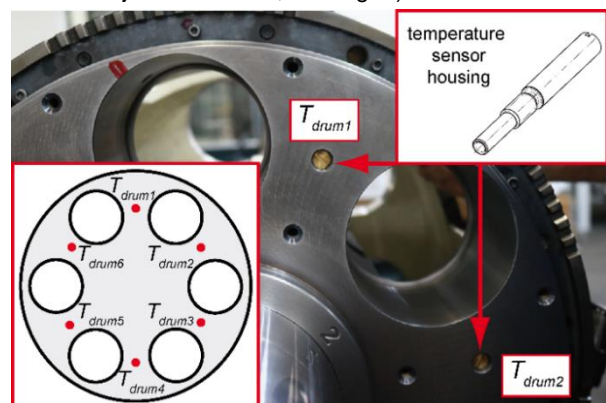


Fig. 3: The temperature sensor housing, the position of the temperature sensors on the spindle drum ( $T_{drum}$ ).

##### Measuring and transmitting unit

The measuring and transmitting unit is intended for data collection from temperature sensors using I<sup>2</sup>C bus and measured data transmission to the receiving and integration unit by Packet Radio (PR) technology (2.4 GHz). The scheme of the measuring and transmitting unit is shown in Fig. 4.

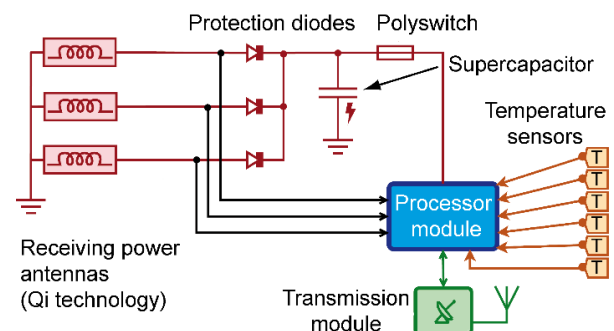


Fig. 4: The scheme of the measuring and transmitting unit.

The measuring and transmitting unit is embedded in a special box made by 3D printing technology, see Fig. 5. Wireless power transfer using inductive charging based on an open interface standard (Qi standard) is employed to power the measuring and transmitting unit. The energy is stored in an internal capacitor (supercapacitor, see Fig. 4).

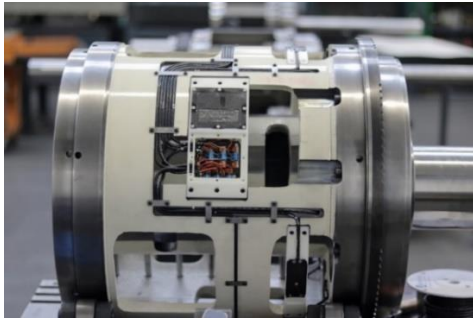


Fig. 5: The measuring and transmitting unit embedded into the special box made by 3D printing technology (white box), the receiving antennas placed on the casting.

The wireless power supply of the measuring and transmitting unit consists of two flat transmitting antennas (fixed on the stationary part of the six-spindle automatic lathe at an angular distance of 180 degrees to each other) and three receiving antennas (placed on the rotating spindle drum at an angular distance of 120 degrees to each other, see Fig. 5). The placement of the two Qi antennas (the transmitting antenna and the receiving antenna) in relation to each other is shown in Fig. 6.

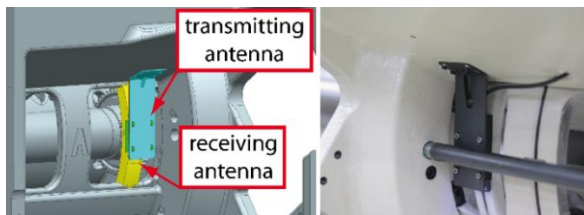


Fig. 6: Proposed placement of the two Qi antennas (left) in relation to each other, implementation (right).

The energy transfer by either of the antennas is sufficient to power the entire measuring system. As long as the drum moves from one fixed position to another, the power supply is provided by the internal supercapacitor.

#### Receiving and integration unit

The principal purpose of the receiving and integration unit is to wirelessly receive measured and service data.

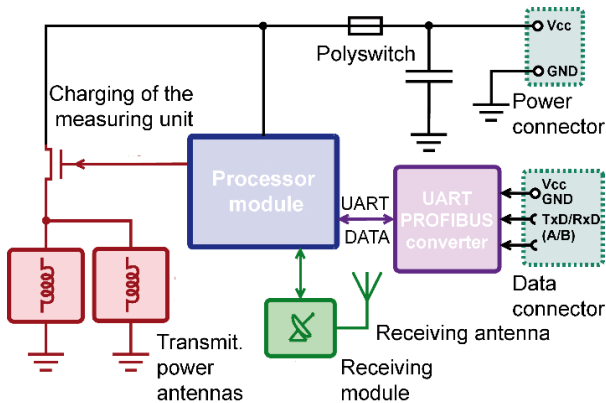


Fig. 7: The scheme of the receiving and integration unit.

The unit's additional functions are charging of the measuring unit and transmitting unit with the above-mentioned Qi technology, transmission of measured data

to the machine tool control system via PROFIBUS, and network communication with the data acquisition system (NI cRIO-9014). The receiving and integration unit scheme is shown in Fig. 7. The implementation of the receiving and integration unit mounted on the six-spindle automatic lathe is shown in Fig. 8.



Fig. 8: The receiving and integration unit mounted on the six-spindle automatic lathe.

## 4 EXPERIMENTS

### 4.1 Experimental setup

The six-spindle automatic lathe was equipped with all smart sensor components outlined in Section 3. Data was acquired during the experiments through the NI cRIO-9014 produced by National Instruments and LabVIEW software. The NI cRIO-9014 collected NC data from the machine tool control system and measured the spindle drum temperature by the smart sensor via PROFIBUS. Moreover, the PAC NI CompactRIO sensed additional external resistance temperature sensors (RTD, Pt100, Class A, 3850 ppm/K). External RTD sensors were placed on the machine tool structure (e.g., the stationary part near the spindle drum  $T_{static}$ , see Fig. 1) and its surroundings (ambient temperature  $T_{amb}$ , see Fig. 1). Generally, the calibration measurement describes a transient characteristic between two thermodynamic equilibria; one with the surrounding of the machine tool and one with all active heat sources which the compensation model should predict (e.g., spindle motors, feed drives, etc.). This kind of machine tool is typically used for one workpiece technology in the long term.

### 4.2 Test piece

The basic scheme of the test piece used for the described experiments is depicted in Fig. 9.

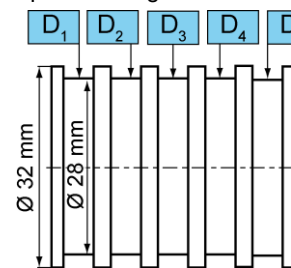


Fig. 9: Test piece.

The diameter denominated as  $D_1$  (28 mm) of the test piece is manufactured at the first MP (MP1) of the six-spindle automatic lathe, the diameter denominated as  $D_2$  of the test piece is manufactured at the second MP (MP2), etc. Thus, test pieces enables to evaluate thermal errors in the X-direction for MP 1 to MP 5. Test piece has no measurable diameter manufactured in MP 6 due to the machine tool builder requirements. The reason is that MP6 is ordinarily used only to cut-off manufactured test pieces from the steel bar of 32 mm diameter (the blank) which is also the last

operation in working cycle of the test piece depicted in Fig. 9. Simple shape of the test piece was selected to ensure same material removal rate in each MP (from MP 1 to MP 5). It should ensure the similar influence of the tool wear, approximately same heat produced in cutting zone in each MP, etc. Test pieces were machined only in certain time intervals during the calibration measurement (due to material savings) otherwise the machine realizes air-cutting with movements analogical to machining of the test pieces in Fig. 9. This time interval was changed according to the actual thermal state of the six-spindle automatic lathe from 5 min (at the beginning of the test) to 30 min (at the end of the test) to obtain transient responses (thermal errors in X-directions) in each MP. The recording of thermal displacements of the examined diameters ( $D_1$  to  $D_5$ ) was obtained by machining the test piece sets in defined time intervals. One set stands for 6 test pieces (one revolution of the spindle drum which lasted 60 s). Thus, several sets of test pieces represent the time axis of the thermal displacements of the machine in the X-direction, see Fig. 10. Subsequently, manufactured 16 sets of test pieces were gauged using an optical measuring system Opticline C305 (Jenoptik) in an air-conditioned room, accuracy (MPE-maximum permissible error) is  $0.3 \mu\text{m}$ , repeated precision is  $0.5 \mu\text{m}$ . Thus, thermal displacements in X-directions are obtained only during the heating phase (16 sets of test pieces represent 5 hours of calibration measurement during the activity of all heat sources caused by the motion of the feed drive axes, spindles, etc.).

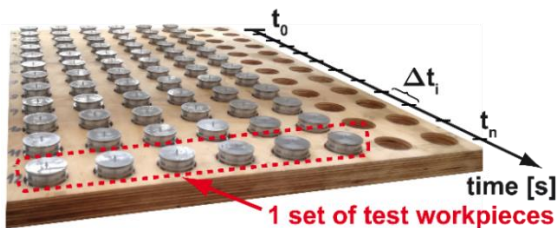


Fig. 10: Several sets of manufactured test pieces.

### 4.3 Experiment results

Fig. 11 depicts the selected temperature behaviour over time during the calibration measurement of the thermal error compensation model. The tests revealed that smart sensor ( $T_{drum}$ ) has the fastest response time in comparison with temperature measured on the stationary part near the spindle drum ( $T_{static}$ , see Fig. 1) and also the temperature placed at the flange of the spindle motor ( $T_{mot}$ , see Fig. 1) which is used as input for previous TF model.

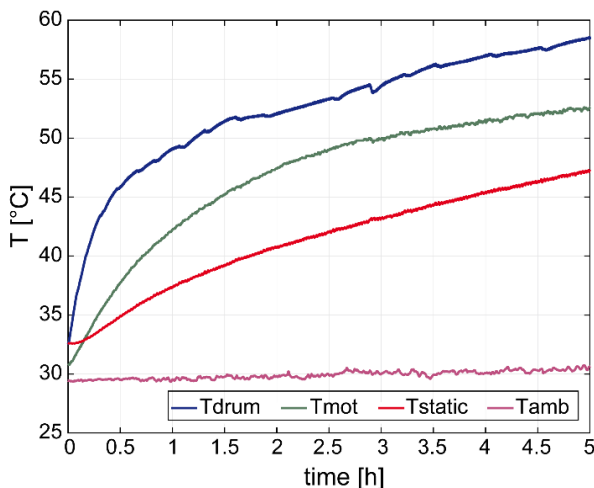


Fig. 11: Selected temperature behaviour over time during calibration measurement.

Sensors  $T_{drum1}$  to  $T_{drum6}$  (see Fig. 3) have very similar temperature behaviour and time response. Thus, the only temperature  $T_{drum1}$  is displayed in Fig. 11 labelled as  $T_{drum}$ . Consequently, the only 1 temperature  $T_{drum1}$  is employed to predict thermal displacements in X-direction for each machining position (MP 1 to MP5), see Section 5. The changes of the test piece diameters  $D_1$  to  $D_5$  over time measured by optical measuring systems are shown in Fig. 12. Since the cutting operations are carried out only during a short period of time to manufacture the test pieces, the influence of tool wear can be neglected. Thus, it can be presumed that the measured changes of the test piece diameters (see Fig. 12) represent thermally induced displacements in different MPs of the six-spindle automatic lathe in the X-direction. The thermally induced displacements in different WP of the six-spindle automatic lathe in the X-direction (uncompensated state of the lathe) are located between  $-60 \mu\text{m}$  and  $+3 \mu\text{m}$ .

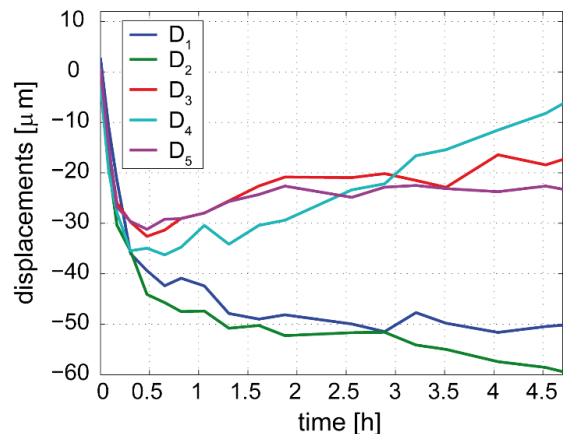


Fig. 12: Thermally induced displacements in the X-direction without thermal compensation.

## 5 RESULTS

The measured data from the calibration measurement presented in Section 4.3 were used to build the thermal error compensation model with the spindle drum temperature  $T_{drum}$  as input, see Fig. 2. Residual thermal errors of the six-spindle automatic lathe in the X-direction after application of the thermal error compensation model based on the TF with the spindle drum temperature  $T_{drum}$  as input are shown in Fig. 13. The compensation model reduced thermally induced displacements in different MPs in the range of  $-13 \mu\text{m}$  to  $+11 \mu\text{m}$ .

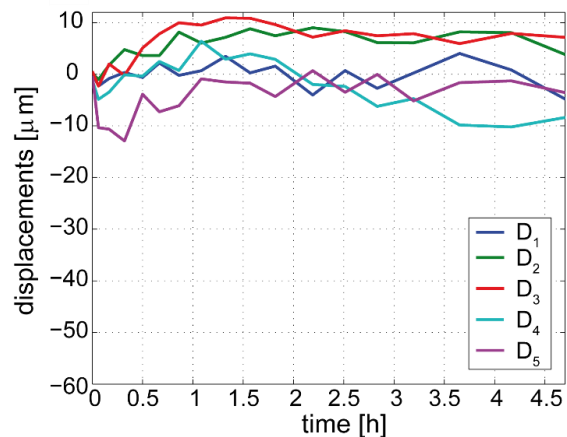


Fig. 13: Residual thermal errors of the six-spindle automatic lathe in the X-direction after the thermal compensation (residual errors of the TF model).

A comparison of both ranges of thermal errors for different MPs without thermal compensation and after application of compensation is carried out in Fig. 14. The light-grey area in Fig. 14 stands for the thermal displacement envelope of the uncompensated state (the maximum thermal displacement in the X-direction is  $-58 \mu\text{m}$ ) and the blue area delineates the envelope of the compensated state.

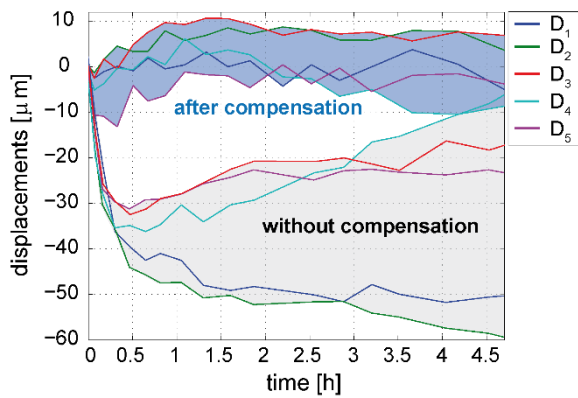


Fig. 14: The comparison of both ranges of thermal errors for different MPs without thermal compensation and after compensation ( $T_{drum}$  as model input).

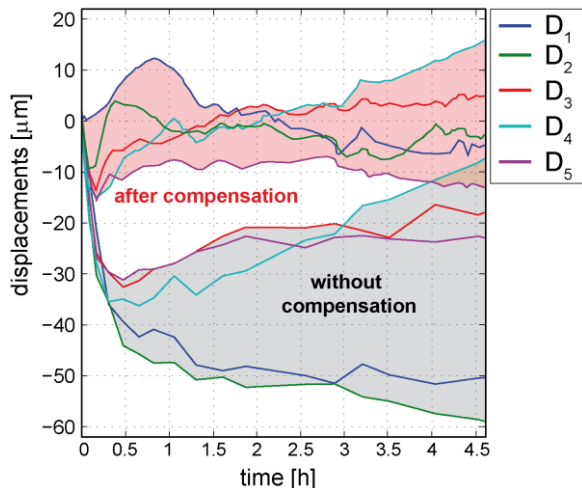


Fig. 15: The comparison of both ranges of thermal errors for different MPs without thermal compensation and after compensation ( $T_{mot}$  as model input).

The analogical graph for the thermal error compensation model with the temperature measured on the stationary part at the flange of the spindle motor ( $T_{mot}$ ) is shown in Fig. 15. The red area delineates the envelope of the compensated state by the compensation model with the temperature measured on the stationary part at the flange of the spindle motor ( $T_{mot}$ ). In this case, the compensation model reduced the thermally induced displacements in different MPs in the range of  $-16 \mu\text{m}$  to  $+17 \mu\text{m}$ . It is evident from a comparison of Fig. 14 and Fig. 15 that the development of the smart sensor and the application of the measured temperature on the rotating spindle drum ( $T_{drum}$ ) as model input results in higher prediction of thermal errors in X-axis in different MPs of the six-spindle automatic lathe. Consequently, the machining accuracy of the six-spindle automatic lathe is highly improved. Furthermore, to verify the quality and robustness of the improved compensation model prediction (model with temperature  $T_{drum}$  as input), three additional experiments were carried out.

One verification test was devised to evaluate the model prediction quality and robustness under continuous

machining, which corresponds to the typical operation of the six-spindle automatic lathe. Firstly, the six-spindle automatic lathe was switched off for at least 12 hours before the continuous machining test. Thus, the lathe cooled down (so that it was practically in thermodynamic equilibrium with its surroundings). Then, the machine tool was powered on and the continuous machining test started immediately. Test pieces according to Fig. 9 were continuously manufactured for 1.6 hours. The continuous machining test results are depicted in Fig. 16.

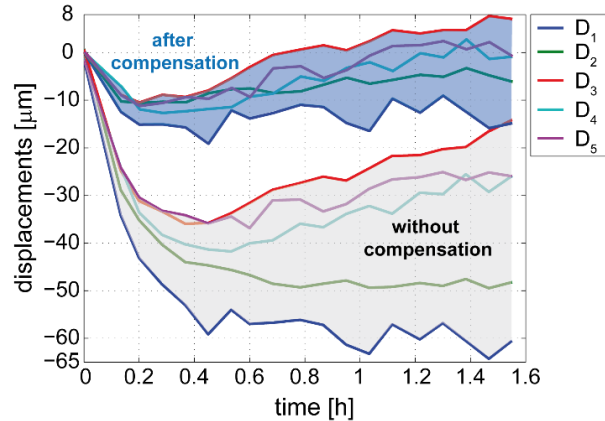


Fig. 16: Results of the continuous machining test.

Thermally induced displacements are in the range of  $-65 \mu\text{m}$  to  $0 \mu\text{m}$  for the uncompensated state of the lathe. The thermal error compensation model based on the TF with the spindle drum temperature  $T_{drum}$  as input reduced thermally induced displacements in different MPs in the range of  $-16 \mu\text{m}$  to  $+17 \mu\text{m}$ . The continuous machining test results confirmed that the accuracy and reliability of the estimated thermal displacements by the compensation model are good even for standard (continuous) six-spindle automatic lathe machining conditions.

The approximation quality of the simulated behaviour can be expressed by the *fit* value, calculated as

$$fit = \left( 1 - \frac{\|\delta_{mea} - \delta_{sim}\|}{\|\delta_{mea} - \bar{\delta}_{mea}\|} \right) \cdot 100. \quad (4)$$

The  $\delta_{mea}$  value in equation (4) is the measured output (thermal displacements in the X-direction,  $\delta_{x,i}$ ),  $\delta_{sim}$  is the simulated/predicted model output, and  $\bar{\delta}_{mea}$  expresses the arithmetic mean of the measured output over time. The vector norm used in equation (4) is generally expressed as follows

$$\|\delta\| = \sqrt{\delta_1^2 + \delta_2^2 + \dots + \delta_r^2}, \quad (5)$$

where  $\delta$  is a general vector of the length  $r$ .

The *fit* values according to equation (4) were calculated for both thermal error compensation models based on the TF ( $T_{mot}$  or  $T_{drum}$  as input, see Fig. 2) for four experiments (one calibration measurement and three verification tests including the continuous machining test). The *fit* values for the calibration test and the continuous machining test for both thermal error compensation models are shown in Tab. 1. The approximation quality expressed by the average *fit* value (from the point of view of the MPs and the performed tests) for the model based on the TF using spindle drum temperature  $T_{drum}$  as input increased by 16% in comparison with the average *fit* value for the compensation model with temperature measured on the stationary part of the six-spindle automatic lathe ( $T_{mot}$ ) as input. A significant reduction of thermal displacements in

the X-direction for all tested MPs of the six-spindle automatic lathe was achieved during all tests (a reduction of 65% expressed by the average *fit* value over all performed tests) due to the compensation model using  $T_{drum}$  as input.

Tab. 1: Results of the compensation model expressed by the *fit* values.

Workpiece Diameter	Calibration test <i>fit</i> [%]		Continuous machining <i>fit</i> [%]
	$T_{drum}$	$T_{static}$	$T_{drum}$
$D_1$	84	66	63
$D_2$	83	76	79
$D_3$	60	63	50
$D_4$	51	7	62
$D_5$	58	44	61
	<b>Average <i>fit</i> [%]</b>		
	67	51	63

## 6 CONCLUSIONS

A novel smart sensor for measuring the spindle drum temperature of a multi-spindle automatic lathe was proposed. The main objective of the smart sensor development was to improve the multi-spindle automatic lathe thermal error compensation model. The spindle drum temperature obtained by the smart sensor was applied as input to the thermal error compensation model based on the TF instead of the original temperature measured on the stationary part of the multi-spindle automatic lathe. This led to a 65% reduction in the thermal displacements in the X-direction for all tested machining positions of the six-spindle automatic lathe in comparison with the uncompensated state. The results of the verification tests confirmed that the accuracy and reliability of the estimated thermal displacements by the compensation model using the spindle drum temperature as the compensation model input are better than the results obtained by the previous compensation model with temperature measured on the stationary part as input. The prediction of thermal displacements in X-axis increased by 16% after the spindle drum temperature was used as the compensation model input instead of the original temperature measured on the stationary part of the machine tool structure. Thus, the thermal error compensation model with the spindle drum temperature measured by the developed smart sensor has a demonstrable benefit compared to the original compensation model. The data presented here underlines that the best excitation of the transfer function model is temperature measured as closed as possible to the relevant heat source. The results are in line with previously published findings. The research also proved that the prediction of the compensation model is more robust even for continuous machining conditions, which correspond to typical six-spindle automatic lathe operations. In addition, it may be presumed that the thermal error compensation model could be applicable to a wider range of working conditions.

## 7 ACKNOWLEDGMENTS

The authors would like to acknowledge funding support from the Czech Ministry of Education, Youth and Sports

under the project CZ.02.1.01/0.0/0.0/16\_026/0008404 "Machine Tools and Precision Engineering" financed by the OP RDE (ERDF). The project is also co-financed by the European Union.

## 8 REFERENCES

- [Horejs 2010] Horejs, O., et al. Compensation of machine tool thermal errors based on transfer functions. *MM Science Journal*, 2010, No.1, pp 162-165.
- [Horejs 2012] Horejs, O., et al. Advanced Modelling of Thermally Induced Displacements and Its Implementation into Standard CNC Controller of Horizontal Milling Center. *Procedia CIRP*, 2012, Vol.4, No.1, pp 67-72
- [Horejs 2013] Horejs, O., et al. Complex verification of thermal error compensation model of a portal milling centre. In: *Proceedings of the International Conference on Advanced Manufacturing Engineering and Technologies (NEWTECH 2013)*, Stockholm, Sweden, 27-30 October, 2012, Vol.1, pp 233-242, ISBN 978-91-7501-892-8
- [Horejs 2014] Horejs, O., et al. A general approach to thermal error modelling of machine tools. In: *Machines et usinage a grande vitesse (MUGV)*, Clermont Ferrand, France, 15-16 October, 2014
- [IEC 60529 2013] IEC 60529: 2013. Degrees of Protection Provided by Enclosures (IP Code). IEC Webstore. <https://webstore.iec.ch/publication/2452>
- [Lasi 2014] Lasi, H., et al. *Industry 4.0. Business & Information Systems Engineering*, 2014, Vol.6, No.4, pp 239-242
- [Li 2018] Li, L. China's manufacturing locus in 2025: With a comparison of "Made-in-China 2025" and "Industry 4.0". *Technological Forecasting and Social Change*, 2019, Vol.135, pp 66-74
- [Liu 2019] Liu, K., et al. Intelligentization of machine tools: comprehensive thermal error compensation of machine-workpiece system. *The International Journal of Advanced Manufacturing Technology*, 2019, Vol. 102, pp 3865-3877.
- [Ljung 2020] Ljung, L. *System Identification Toolbox™ User's Guide*. The MathWorks, 2015. [https://ch.mathworks.com/help/pdf\\_doc/ident/ident\\_ug.pdf](https://ch.mathworks.com/help/pdf_doc/ident/ident_ug.pdf)
- [Mayr 2012] Mayr, J., et al. Thermal issues in machine tools. *CIRP Annals - Manufacturing Technology*, 2012, Vol.61, No.2, pp 771-791, ISSN 0007-850
- [Mares 2014] Mares, M., et al. Approach to thermal error modeling and compensation of a six-spindle automatic lathe. In: *Machines et usinage a grande vitesse (MUGV)*, Clermont Ferrand, France, 15-16 October, 2014
- [Mares 2020] Mares, M., et al. Thermal error compensation of a 5-axis machine tool using indigenous temperature sensors and CNC integrated Python code validated with a machined test piece. *Precision Engineering*, November 2020, Vol.66, pp 21-30
- [Microchip 2011] Microchip Technology. MCP9808. 2011. <https://www.microchip.com/wwwproducts/en/en556182>
- [National Instruments 2016] National Instruments. *User manual and specifications NI cRIO-9012/9014*. 2016. <https://www.ni.com/pdf/manuals/374126g.pdf>
- [TAJMAC-ZPS 2020] TAJMAC-ZPS. Six-spindle automatic lathe MORI-SAY TMZ642CNC. 2020. <https://www.tajmac-zps.cz/vicvretrenovy-soustruznicky-automat-mori-say-tmz642cncen>